Fuel 312 (2022) 122896

Contents lists available at ScienceDirect

Fuel

journal homepage: www.elsevier.com/locate/fuel

Full Length Article

Experimental determination of dissociation temperatures and enthalpies of methane, ethane and carbon dioxide hydrates up to 90 MPa by using a multicycle calorimetric procedure

María Dolores Robustillo [a,b,1,*], Davi Eber Sanches de Menezes [b,c,1], Pedro de Alcântara Pessôa Filho [b]

[a] Departamento de Ingeniería Química Industrial y Medio Ambiente, Escuela Técnica Superior de Ingenieros Industriales, Universidad Politécnica de Madrid, José Gutiérrez Abascal 2, 28006 Madrid, Spain
[b] Department of Chemical Engineering, Engineering School, University of São Paulo (USP), Av. Prof. Luciano Gualberto, 380, 05508-010 São Paulo, SP, Brazil
[c] CEPETRO/FEM, University of Campinas (UNICAMP), PO Box 6052, 13083-896 Campinas, São Paulo, Brazil

ARTICLE INFO

Keywords:
Gas hydrates
High-pressure microcalorimetry
Multicycle method
Enthalpy
Equilibrium properties

ABSTRACT

This work presents the application of a multicycle procedure to determine the dissociation temperature and enthalpy of gas hydrates using high-pressure microcalorimetry (HP-μDSC). In the multicycle procedure, a sample of water in contact with the gas undergoes successive cooling and warming cycles below hydrate dissociation temperature, increasing the conversion of water into hydrate. This technique has been previously used in literature to increase water conversion during carbon dioxide hydrate formation up to 2.0 MPa, but its applicability has not been assessed for higher pressures and with different guest molecules. New experimental equilibrium data for methane, ethane, and carbon dioxide hydrates were obtained through HP-μDSC up to 90 MPa using the multicycle procedure. The advantages and limitations of the method are discussed. Dissociation temperatures are in good agreement with data previously obtained from a HP-μDSC standard method, which confirms the reliability to determine this property by both methods. Nevertheless, the enthalpy of hydrate dissociation obtained by the direct integration of thermograms provided by the HP-μDSC standard method is not accurate. Thus, it is usually calculated by using the Clapeyron equation from equilibrium temperature and pressure data obtained by the HP-μDSC standard method, as presented in previous work. The new dissociation enthalpies presented in this work were obtained experimentally by direct integration of thermograms using the multicycle procedure, which provides accurate data as the conversion is very high (above 97% of water converts into hydrate), the baselines are clearly established, and no exothermic peak related to metastable phases is observed.

1. Introduction

Gas hydrates or clathrates are compounds in which water molecules are bound by hydrogen bonds forming a thermodynamically stable crystalline structure with the inclusion of small gas molecules (guest) in the cavities. Clathrates have received much attention in recent years as advanced materials for storage and transportation of natural gas [58,29], since under standard conditions, 1 m^3 of gas hydrate can store between 150 and 180 m^3 of natural gas [36,50]. Gas hydrates have also received attention as a new method of storage and transportation of hydrogen [16,33,19,72]. They are also attractive to be used in the capture and sequestration of CO_2 [15,60,61,37], water desalination [32,3] and as phase change materials for refrigeration [13,43,44]. They are also important in geophysical and astrophysical areas, where the dissociation of clathrate hydrates has long been inferred as a potential replenishment mechanism for atmospheric methane [45,7,52]. Despite the variety of applications related to sustainable chemistry [29], gas hydrates can be a problem for petroleum companies because their solid character can lead to flow assurance problems. Finally, the melting of permafrost areas due to global warming can release methane trapped

* Corresponding author at: Departamento de Ingeniería Química Industrial y Medio Ambiente, Escuela Técnica Superior de Ingenieros Industriales, Universidad Politécnica de Madrid, José Gutiérrez Abascal 2, 28006 Madrid, Spain.
E-mail address: mariadolores.robustillo@upm.es (M.D. Robustillo).
[1] These authors contributed equally to this work.

https://doi.org/10.1016/j.fuel.2021.122896
Received 9 October 2021; Received in revised form 25 November 2021; Accepted 7 December 2021
Available online 21 December 2021

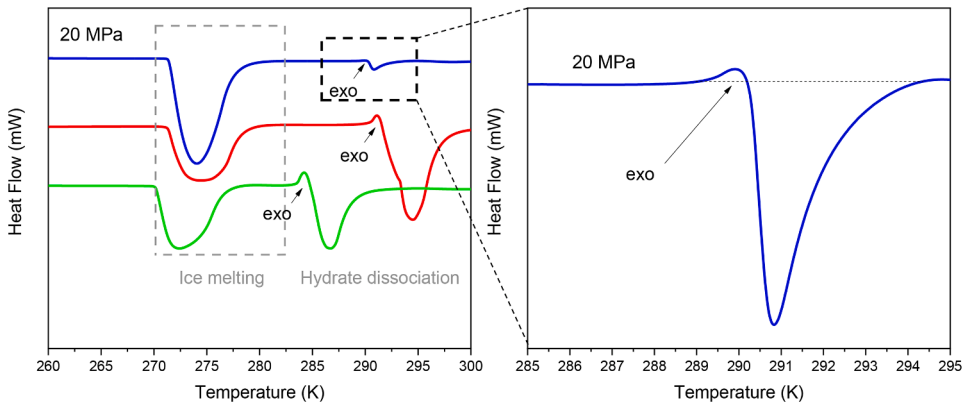

Fig. 1. Thermograms of ethane (——), methane (——) and carbon dioxide (——) hydrates showing the exothermic peak close to the main hydrate dissociation peak. Samples were analyzed at 20 MPa through a standard DSC procedure using cooling and heating rates of 1 K·min^{-1}.

into the hydrate reservoir and produce catastrophic environmental consequences.

Equilibrium (temperature and pressure of dissociation) and thermal properties of gas hydrates (enthalpy of dissociation and heat capacity) are relevant in all these areas. This is true especially when hydrate is proposed to be used as an alternative fuel or in carbon dioxide sequestration and long-term storage in deep-sea sediments, since they provide information about the conditions at which gas hydrate are formed and allow quantify either the amount of energy that can be stored in the hydrate form or the effects on climate change due to hydrate dissociation [22]. Clathrate formation usually requires high pressures, low temperatures, and a high amount of hydrocarbon dissolved in water, conditions that hinder their study due to the necessity of suitable instruments of analysis. Under these conditions, thermal and equilibrium properties of clathrates are scarce, sometimes even inexistent, and mostly derived from mathematical models. The scarcity of experimental equilibrium data available in the literature prevents validation and improvement of the thermodynamic models used in processes design.

The phase behavior of gas hydrates has been extensively studied so far mainly using PVT cells equipped with see-through windows for visual inspection and temperature/pressure sensors for detecting pressure or temperature drop when gas hydrate is formed. However, these experiments are more time-consuming methods and less powerful compared to those based on calorimetry [10]. High-pressure microcalorimetry is a technique that has been used for several years in studies of gas hydrates [28,25,56,41,31,55,9,22,48,51,49,47,46]. It allows to accurately obtain the enthalpy and temperature of any transition involving energy transfer. In pioneering works, gas hydrates were synthesized in a reactor and then transferred into the calorimetric vessel to determine the heat of dissociation and heat capacity [26,23,24,25,56,27,41,31]. However, gas hydrates can be dissociated and contaminated when transferred to the calorimetric cell, and for that reason, in situ formation and characterization of gas hydrates is preferred. Mu and von Solms [51] studied dissociation enthalpies and thermal equilibrium properties of methane-carbon dioxide double hydrates below 10 MPa through microcalorimetry. A high sub-cooling degree is necessary for gas hydrate formation, producing ice, which crystallizes much easier than hydrate [10]. Mass transfer resistance can be reduced (and consequently a higher conversion of water to hydrate can be achieved) if pure water is injected into three capillary tubes with a micro-syringe [51]. However, even with this method, some of the dissociation thermograms still present a small exothermic peak closely behind the main peak. These exothermic signals have also been observed by our group when samples are analyzed through a standard DSC procedure (see Fig. 1).

Mu and Solms [51] attributed this phenomenon to the existence of more than one guest molecule in hydrate structures. Nevertheless, such hypothesis does not explain the presence of these peaks in single guest hydrates formed from one type of gas molecule. Gupta et al. [22] suggested that a similar peak appeared in their work due to the conversion of some melted ice into methane hydrate, which leads to the formation of hydrate metastable phases.

The structure of clathrate hydrates is stabilized as the cage occupancy is increased. The existence of empty cages results in metastable phases which may dissociate in a large range of temperature and influence the enthalpy of dissociation values and equilibrium properties. These factors can lead to considerable uncertainties in these measurements. The use of a multicycle program of temperature, as described in Delahaye et al. [12], constitutes an alternative to reduce the appearance of metastable hydrate phases. The multicycle method consists of successive cooling and warming cycles below hydrate dissociation temperature, allowing water consumption to be monitored by the decrease in the ice melting peak at constant pressure. Once this signal is almost negligible, or its enthalpy becomes constant, which means that the amount of ice in the system is low or inexistent, the maximum conversion of water into gas hydrate has been reached and any metastable phase has disappeared. Thus, no recrystallization peak is observed, and the concentration of produced hydrate sample is maximized. Hence, the signal-to-noise ratio (sensitivity) and resolution (degree of separation of overlapping thermal effects from each other) increase. Consequently, the integration of dissociation peak to determine enthalpy and equilibrium properties is more accurate than in the standard procedure.

The multicycle method has been successfully used to analyze carbon dioxide hydrates up to 20 MPa [42]. Few hours were necessary to convert water into hydrate. However, the formation of cyclopentane hydrates at atmospheric pressure was not observed through this methodology after more than 60 h of experiment [66]. Since the rate of hydrate formation is limited by gas–liquid mass transfer, increasing pressure and/or mixing is required in this case. A novel prototype of a mixing cell has been recently designed for microcalorimetry measurements on gas hydrates to improve mass transfer and promote clathrate formation [66]. Nevertheless, their maximum working pressure is 15 MPa. Thus, the multicycle protocol is currently the only alternative to measure properties reliably above this threshold. However, the existing studies are restricted to CO_2 hydrates at pressures below 20 MPa. To evaluate the applicability of the multicycle DSC technique to a greater number of systems and pressure ranges, in this work equilibrium and thermal properties of methane, ethane and carbon dioxide single guest hydrates have been studied up to 90 MPa by high-pressure microcalorimetry. Both multicycle equilibrium temperatures and enthalpies obtained herein were compared with data reported in previous work, in which the standard DSC method was applied to experimentally determine equilibrium temperatures, and enthalpies were calculated solely through the Clapeyron equation [46]. Since enthalpy determination

Table 1
Samples used in microcalorimetric analyses.

Component	CAS Registry Number	Source	Purity[a] (mol%)
Naphthalene [b] ($C_{10}H_8$)	91-20-3	Setaram	≥ 99.97
Methane (CH_4)	74-82-8	White Martins	≥ 99.50
Ethane (C_2H_6)	74-84-0	Linde	≥ 99.95
Carbon Dioxide (CO_2)	124-38-9	Gama	≥ 99.99

[a]As reported by the supplier. [b] Used for the instrument calibration and certified by LGC organization.

requires the knowledge of the water to guest ratio (hydration number, *n*), two recently developed approaches [46] were used to determine this parameter. The first one is based on the fractional cage occupancy parameter, which is predicted by the CSMGem software assuming one guest per cavity. The second one is based on an iterative method that considers the hydrate dissociation enthalpy variation between two points related to experimental conditions. Further details about both methods can be obtained in Menezes et al. [46] and are briefly described in section 2.6. The effects of isothermal compressibility and isobaric expansivity on the lattice parameter were considered to estimate the hydrate volume. A detailed description of the procedure is described in Menezes et al. [46].

2. Experimental Configuration and Methods

2.1. Material

The specification of the gases used in gas hydrates studies is presented in Table 1. Milli-Q water, ranging from 30 to 65 mg, was used in all the analyses performed by the high-pressure microcalorimeter.

2.2. Experimental configuration

Dissociation temperature and enthalpies of gas hydrates were measured by a high-pressure microcalorimeter (μ-DSC7 evo - Setaram). A temperature correction coefficient based on the well-known melting properties of different substances (naphthalene, water and n-decane) and a Joule effect calibration of the sensitivity coefficient (which converts the electrical energy into heat flow) were performed at the manufactureŕs factory. Calibration was checked according to the manufacturer's recommendations, by using high purity naphthalene (≥99.97%) and hermetically sealed standard cells. Experimental high-pressure cells (measurement and reference), made of Incoloy and with a maximum volume available for the sample of 0.19 mL, were placed inside two block-machined cavities of the furnace. The reference cell remained empty and depressurized during the whole experiment. The double-stage temperature control with Peltier coolers allows the equipment to work from 228.15 K to 393.15 K, aided by an auxiliary thermostatic bath Julabo F32. The resolution of the calorimeter is 0.02 μW. A constant flow of inert gas (nitrogen 99.999%) was used to avoid water condensation in the calorimetric wall, especially at low temperatures. A gas mixer and a high-pressure piston compressor were connected to the microcalorimeter to prepare gas mixtures (when necessary) and to control the pressure, respectively. This configuration allows operation at constant pressure or constant volume at pressures up to 100 MPa with an accuracy of ± 0.2 MPa. The possibility of humidity condensation over the DSC components when working at sub-ambient temperatures was reduced by introducing the calorimeter inside an acrylic box with a constant flow of dry air. A scheme of the experimental configuration is shown in Fig. 2.

2.3. Standard and multicycle methods

The standard experimental procedure is described in previous works [48,49,47,46]. The sample was first cooled at 1 K/min from 293.15 K to 233.15 K at constant pressure to form the methane hydrate, and after 10-min of equilibration time at the lowest programmed temperature (233.15 K) the hydrate sample is subsequently heated until its dissociation. During the multicycle procedure, the sample is also cooled at the

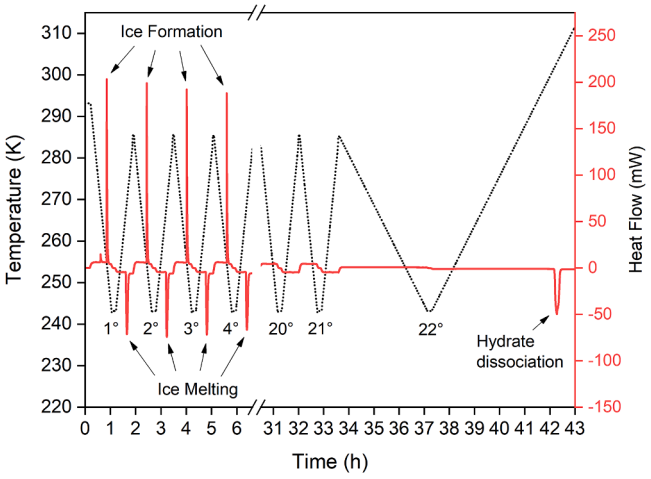

Fig. 3. Example of a multicycle procedure applied to increase the conversion of water into CH_4 hydrate at 70 MPa.

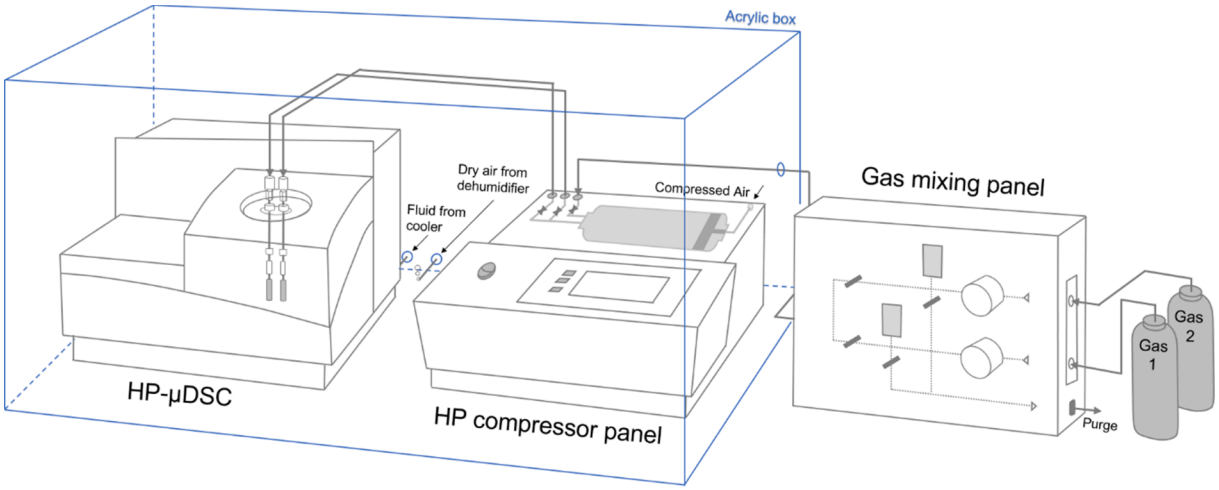

Fig. 2. Instrument setup for calorimetric measurements [45].

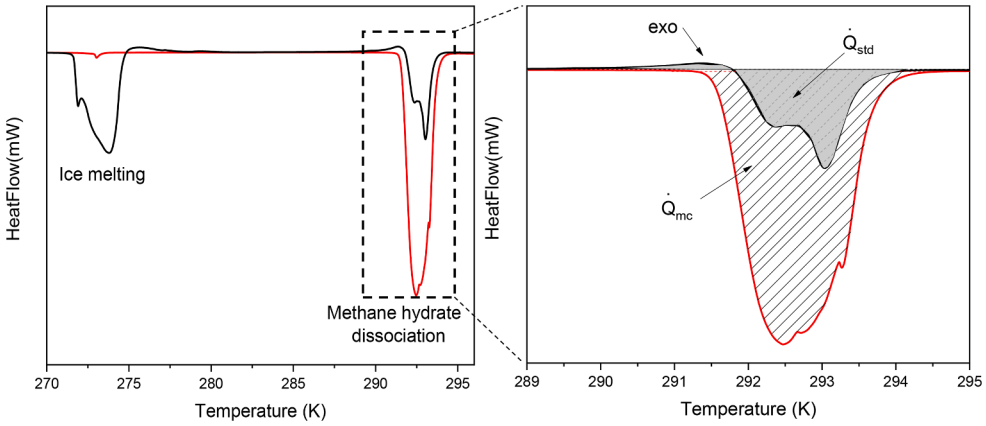

Fig. 4. Heating thermograms of methane hydrate obtained by the standard DSC method (▬▬) and the multicycle method (▬▬). Samples were analyzed at 20 MPa using a cooling and a heating rate of 0.2 K·min^{-1}; *std*: standard method; *mc*: multicycle method.

same conditions as in the standard procedure, and heated until the non-converted ice is melted, but without dissociating the formed hydrate in each cycle, as illustrated in Fig. 3. This temperature is previously estimated from the standard analysis and should be at least 5 K higher than the ice melting endset temperature or more if the ice melting and hydrate dissociation peaks are separated enough. Consecutive cooling-heating cycles are repeated until the water conversion into hydrate is higher than 97% after the last cycle. Once the conversion threshold is reached, the sample is heated during the last cycle until total dissociation of clathrate and equilibrium properties are obtained from the dissociation peak. Calisto software (Setaram) was used to determine onset, peak and endset points, as detailed in previous work [46].

2.4. Dissociation enthalpy based on integration of thermograms

The methodology to determine the dissociation enthalpy was firstly applied for methane hydrate by Gupta et al. [22] by using the high-pressure microcalorimetric standard method. In this work, the calculation procedure of Gupta et al. [22] was extended to higher pressures (up to 90 MPa) and different guest molecules. However, the direct integration of hydrate dissociation curves obtained with the standard method may not provide accurate enthalpy values for ethane and carbon dioxide hydrates, as they remain in the liquid phase. In a single standard experimental run, the conversion of water into hydrate is incomplete, and so the total heat absorbed to dissociate the hydrate ($\dot{Q}$, $mW{\cdot}K$) cannot be directly used to calculate the dissociation enthalpy, as will be described later. The higher the amount of non-converted water into hydrate, the higher the uncertainty. Nevertheless, the integration of the hydrate dissociation peak obtained by the multicycle method, as illustrated in Fig. 4, provides the total heat absorbed during dissociation ($\dot{Q}$, $mW{\cdot}K$) regardless of the guest molecule used to form the hydrate, since no free water or ice is practically present in the system. The dissociation enthalpy per mol of gas (ΔH_{diss}, $J{\cdot}mol^{-1}$) is obtained through Eq. (1), wherein $\varnothing$ is the heating rate ($K{\cdot}min^{-1}$).

$$\Delta H_{diss} = \frac{\dot{Q}_{hydrate\ dissociation}}{n_{gas}{\bullet}\varnothing} \tag{1}$$

Fig. 4 compares heating thermograms of methane hydrate obtained by the standard DSC method and the multicycle method. Differences between hydrate dissociation peaks areas are remarkable. Exothermic transition is only observed when the standard method is used.

For methane hydrate, for instance, the reaction of formation is presented in Eq. (2), in which (n) is the hydration number:

$$CH_4 + nH_2O \rightarrow CH_4{\bullet}\mathrm{nH_2O} \tag{2}$$

The amount of gas incorporated in the hydrate (n_{gas}) can be estimated by considering the amount of water in the form of hydrate (Eq. (3)) and the stoichiometric ratio determined by the hydration number (n). Estimations of the hydration number can be found in the literature [62,64]. For methane hydrate, the value for n is close to 6 [8,28], but a wider range of values is found in the literature for carbon dioxide hydrates. Moreover, the hydration number may depend significantly on the pressure. The methods to estimate values of hydration number are described in section 2.6.

The amount of water in the form of hydrate, $n_{H_2O(hidrate)}$, can be obtained by Eq. (3), because the total amount of water initially added in the cell is known. When a peak is found at the ice melting temperature, the amount of water not converted to hydrate is calculated by integrating this peak (Eq. (4)). Since the amount of water in the calorimetric cell is very low (30–65 mg), it is considered that the amount of gas dissolved in the water at the experimental conditions is negligible, according to Mu and von Solms [51]. The melting enthalpy of ice was extrapolated to the specific system pressure [6,14,20,34].

$$n_{H_2O\ (hydrate)} = n_{H_2O\ (total)} - n_{H_2O\ (ice)} \tag{3}$$

$$n_{H_2O\ (ice)} = \frac{\dot{Q}_{Ice\ melting}}{\Delta H_{Ice\ melting\ (theorical)}{\bullet}\varnothing} \tag{4}$$

The advantage of the multicycle method is that none or a small fraction of water is present during the last cycle and no metastable hydrate phases are formed. The integration of the hydrate dissociation peak provides a representative value of the total heat absorbed during dissociation ($\dot{Q}$, $mW{\cdot}K$). This fact contributes to a higher analytical accuracy.

2.5. Dissociation enthalpy based on the Clapeyron equation

The enthalpy of dissociation at each point was calculated based on the Clapeyron equation (Eq. (5)). The experimental equilibrium temperature (T,K) and pressure (P,MPa) obtained by the multicycle method were fitted to polynomial equations, as presented in Appendix A. The expressions of dP/dT were obtained by simple derivation. Following Anderson approach [1,2], the volume change, ΔV ($m^3{\bullet}\mathrm{mol}^{-1}$), was calculated through equation (6), considering the compounds and phases involved: hydrocarbon or CO_2 (V_{HC} or V_{CO_2}; vapor or liquid), water (V_{H_2O}; ice or liquid) and hydrate (V_{hyd}; solid).

$$\frac{dP}{dT} = \frac{\Delta H}{T\Delta V} \tag{5}$$

$$\Delta V = \left(1 - \frac{n{\bullet}x_{HC}}{1 - x_{HC}}\right){\bullet}\mathrm{V_{HC}} + \mathrm{n}{\bullet}\left(\mathrm{V_{H_2O}} + \left(\frac{\mathrm{x_{HC}}}{1 - \mathrm{x_{HC}}}\right){\bullet}\mathrm{V^{\infty}_{HC,H_2O}}\right) - \mathrm{V_{hyd}} \tag{6}$$

Table 2
Reproducibility of dissociation data of CH_4 hydrates obtained at 20 MPa by HP-μDSC* using the multicycle method.

P (MPa)	n° Cycles	Ø (K·min^{-1})	H_2O (mg)	H_2O Conv. (%)	T $_{ONSET}$ (K)	T $_{PEAK}$ (K)	T $_{ENDSET}$ (K)	△$H_{integration}$*** (kJ/mol CH_4).	△$H_{Clapeyron}$*** (kJ/mol CH_4).
20	22	0.2	41.6	99.02	291.60	292.48	293.69	55.26	54.23
	27**	0.2	47.0	99.20	291.70	293.77	294.69	55.18	54.94
	22	0.2	56.5	98.87	291.74	293.25	294.81	55.75	54.97

* – Standard uncertainties are u(T) = 0.3 K, u(x) ≈ 0.0002 and u(P) = 0.1 MPa.
** – water conversion after 22 cycles was 98.3%.
*** – Hydration number obtained from iterative method (n = 6.17).

Table 3
Dissociation data of CH_4 hydrates obtained by HP-μDSC* using standard and multicycle methods.

P (MPa)	n° Cycles	Ø (K·min^{-1})	H_2O (mg)	H_2O Conv. (%)	T $_{ONSET}$ (K)	T $_{PEAK}$ (K)	T $_{ENDSET}$ (K)
9.8	1	1	56.5	–	285.87	288.25	290.20
	23	0.2	56.5	97.96	285.94	288.13	289.57
20	1	0.2	31.0	–	291.74	292.92	293.91
	1	1	41.6	–	291.43	292.44	294.53
	22	0.2	41.6	99.02	291.60	292.48	293.69
	1	1	56.5	–	291.56	294.49	296.92
	22	0.2	56.5	98.87	291.74	293.25	294.81
31.5	1	1.0	56.5	–	294.95	297.48	300.41
	17	0.2	56.5	97.62	295.23	296.95	298.17
40	1	0.2	31.0	–	296.98	298.39	299.31
	1	1	56.5	–	296.71	299.37	302.21
	20	0.2	56.5	98.26	296.96	298.63	300.01
50	1	1.0	64.6	–	298.55	300.33	302.20
	22	0.2	64.6	97.51	298.82	300.45	301.19
59.4	1	1.0	41.6	–	300.10	301.25	303.00
	22	1.0	41.6	99.86	299.99	302.03	306.54
70	1	1.0	51.7	–	301.73	302.72	304.44
	22	0.2	51.7	99.83	301.83	302.93	304.43
80	1	0.2	31.1	–	303.21	303.73	304.38
	1	1	64.6	–	302.91	304.79	306.61
	20	0.2	64.6	99.97	303.13	304.33	305.75
90	1	1.0	64.6	–	304.10	305.04	307.03
	15	0.2	64.6	99.98	304.33	305.74	306.44

* – Standard uncertainties are u(T) = 0.3 K, u(x) ≈ 0.0002 and u(P) = 0.1 MPa.

The molar volumes of pure compounds, V_{HC} and V_{H_2O}, were obtained from the NIST Webbook database [59,18,63]. Equation (6) requires the volumes of methane, ethane, and carbon dioxide in water at "infinite dilution" (V^{∞}_{HC,H_2O}) and the enthalpy of solution at infinite dilution ($\Delta H^{\infty}_{HC,H_2O}$) [1,2]. The solubilities of methane and ethane in water (x_{HC}) were determined through the Krichevsky-Kasarnovsky equation [39], while the solubility of carbon dioxide in water was calculated by the correlations from Diamond and Akinfiev [17]. The volume of hydrate containing 1 mol of the guest compound was calculated through equation (7). The calculation of the molar volume of the hydrate unit cell (V_{uc}) accounts for the isobaric thermal expansivity ($\beta_{(v)}$) and isothermal compressibility ($\kappa_{T(v)}$). Details of these calculations are presented in Appendix B.

$$V_{hyd}(T,P)/(m^3 \bullet mol^{-1}) = \frac{6.0221 \bullet 10^{23} \bullet V_{uc} \bullet n}{46} \quad (7)$$

2.6. Estimation of hydration number

The hydration number indicates the number of water molecules per guest molecule. Two methods to estimate n at each experimental point were presented in previous work [46]. A brief description is summarized below to indicate the main equations applied in both methods.

2.6.1. Hydration number based on computational predictions

The first method is based on the software CSMGem predictions and considers the fractional occupancy (θ) for hydrate cavities, which is calculated as a function of the Langmuir constant for the guest molecule in the respective cavity type and of the fugacity of the guest molecule in the gas phase [62]. Considering that the single hydrates studied are known to form structure I, the hydration number can be calculated according to equation (8).

$$n = \frac{46}{2\theta_{small} + 6\theta_{large}} \quad (8)$$

2.6.2. Hydration number by numerical iterations

The second method is based on an iterative procedure to determine the hydration number at different experimental points, not necessarily referring to the lower quadruple point (Q1), as addressed in the literature [11,62]. Considering two points defined by (T_1, P_1) and (T_2, P_2), the hydration number can be estimated by iterations based on Eq. (9). The enthalpy of the dissociation at any point 1 (ΔH_1) is initially calculated by the Clapeyron equation (Eq. (5)), considering a hypothetic value of n. The enthalpy of the hydrate dissociation at point 2, in turn, is found in the literature for the respective system. The enthalpies of hydrocarbons and water (H_{HC} and H_{H_2O}) are taken directly from NIST Webbook. The hydration number obtained is used to recalculate ΔH_1 (Eq. (5)) and the cycle is repeated through iterations until the hydration number

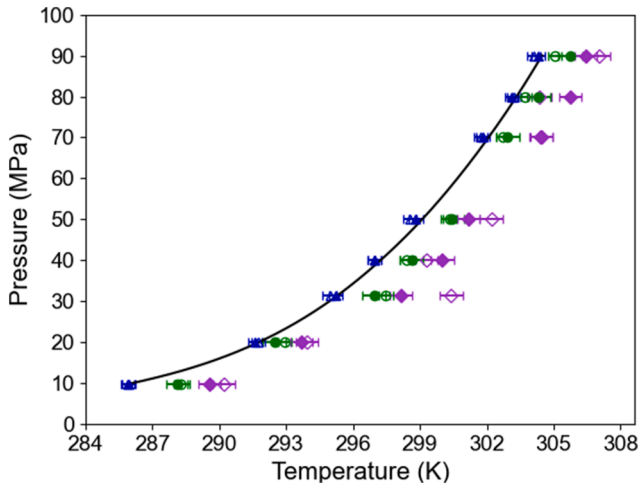

Fig. 5. Dissociation data of CH_4 hydrates obtained by HP-μDSC using standard method (empty symbols) and multicycle method (full symbols) at 0.2 K·min^{-1}: (●) onset temperature; (◆) peak temperature; (▲) endset temperature. Black lines refer to CSMGem predictions. Horizontal lines on the symbols represent the error bars.

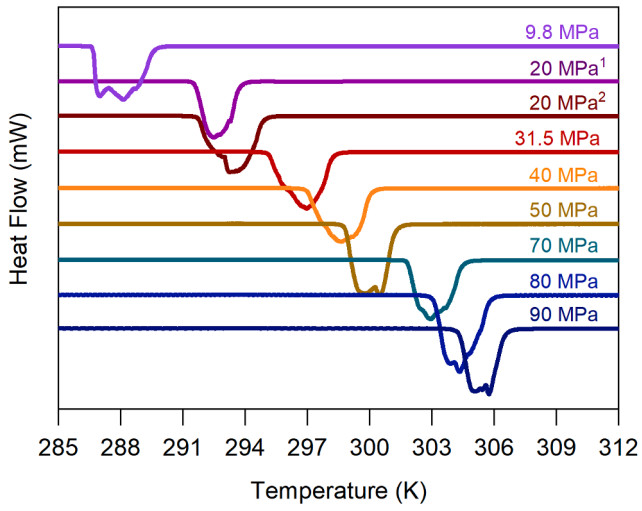

Fig. 6. Thermograms of CH_4 hydrates dissociation obtained by the multicycle method. Two samples were analyzed at 20 MPa containing 41.6 mg[1] and 56.5 mg[2] of water inside the cell.

converges. The calculation of the hydrate enthalpy variation $(H_{Hyd_{(2)}} - H_{Hyd_{(1)}})$ is based on the definition of partial derivatives, as explained in detail in the referred work [46].

$$n = \frac{\Delta H_1 - \Delta H_2 + (H_{HC_{(2)}} - H_{HC_{(1)}}) + (H_{Hyd_{(1)}} - H_{Hyd_{(2)}})}{(H_{H_2O_{(1)}} - H_{H_2O_{(2)}})} \quad (9)$$

2.7. Computational predictions

The equilibrium state of gas hydrates was calculated by the software package CSMGem code Version 1.10 (January 1, 2007). This software package uses the SRK equation of state for liquid and vapor phases and the van der Waals and Platteeuw model for the hydrate phase [69].

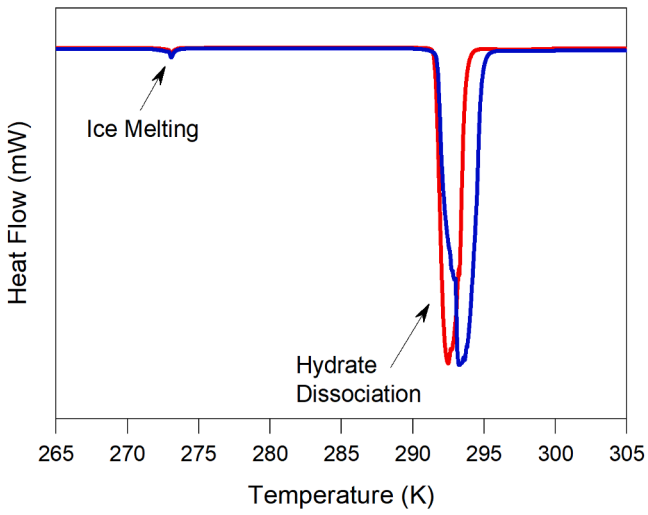

Fig. 7. Dissociation of CH_4 hydrates obtained by the multicycle method at 20 MPa and 0.2 K·min^{-1}: (▬) 41.6 mg H_2O; (▬) 56.5 mg H_2O.

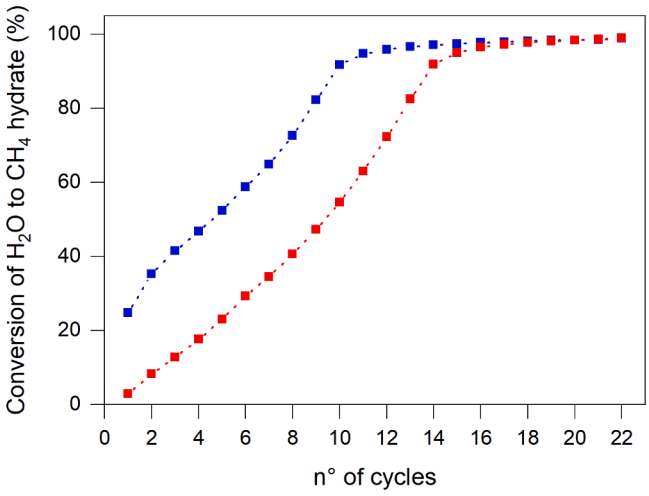

Fig. 8. Conversion of water to CH_4 hydrate throughout 22 cycles at 20 MPa and 0.2 K·min^{-1}: (■) 41.6 mg H_2O; (■) 56.5 mg H_2O.

3. Results

3.1. Methane-Water system

3.1.1. Equilibrium data of CH_4 hydrates

Reproducibility of the multicycle method concerning the water sample size was assessed at 20 MPa. Results shown in Table 2 show no significant difference in onset temperature and enthalpy values, whereas peak and endset temperatures are only slightly influenced by the mass of the water sample.

Table 3 and Fig. 5 present the dissociation data from standard and multicycle methods at several pressures. The onset temperatures agree even when the experiments were carried out at different heating rates. According to Fig. 5, the deviations of onset temperatures and predictions are similar for both standard and multicycle methods and are within the experimental uncertainty.

The onset temperatures obtained by both standard and multicycle methods are in good agreement regardless of the heating rate. Results are also in agreement with Menezes et al. [46]. The values obtained from multicycle experiments seem to be slightly lower than those obtained through the standard method when both methods were performed at the same temperature scanning rate (20, 40 and 80 MPa at 0.2 K·min^{-1};

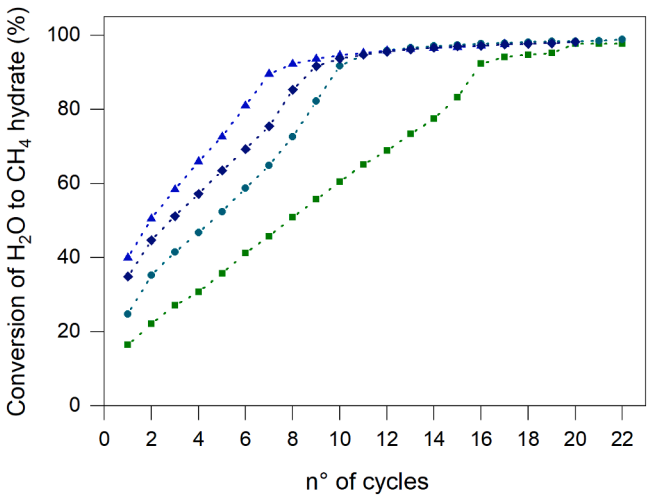

Fig. 9. Effect of pressure on the water conversion to CH_4 hydrate: (■) 9.8 MPa; (●) 20 MPa; (▲) 31.5 MPa; (◆) 40 MPa. All samples consisted of 56.5 mg of water.

Table 4
Enthalpies of CH_4 hydrates based on experimental data obtained by HP-μDSC*.

Hydration number (n) based on predictions of fractional cages occupancy				
P (MPa)	T (K)	n	△H Clapeyron. (kJ/mol CH_4)	△H Integration (kJ/mol CH_4)
20.0	291.74	5.93	55.83	53.61
31.5	295.23	5.89	55.78	53.96
40.0	296.96	5.87	56.28	53.49
50.0	298.82	5.85	56.97	52.99
59.4	299.99	5.83	58.03	53.12
70.0	301.83	5.82	57.98	53.29
80.0	303.13	5.81	58.66	53.05
90.0	304.33	5.80	59.68	-
Multicycle Method (Average ± $CI_{95\%}$)		5.85 ± 0.03	57.40 ± 0.98	53.36 ± 0.26
Standard Method (Average ± $CI_{95\%}$)		[a] 5.85 ± 0.05	[a] 57.72 ± 2.39	53.70 ± 1.50
Hydration number (n) from Iterative Method				
P (MPa)	T (K)	n	△H Clapeyron. (kJ/mol CH_4)	△H Integration (kJ/mol CH_4)
20.0	291.74	6.17	54.97	55.75
31.5	295.23	6.08	54.73	55.67
40.0	296.96	6.09	54.77	55.51
50.0	298.82	6.10	54.92	55.31
59.4	299.99	6.15	55.07	56.06
70.0	301.83	6.09	55.20	55.81
80.0	303.13	6.11	55.37	55.78
90.0	304.33	6.13	55.77	-
Multicycle Method (Average ± $CI_{95\%}$)		6.11 ± 0.02	55.10 ± 0.24	55.70 ± 0.18
Standard Method (Average ± $CI_{95\%}$)		[a] 6.10 ± 0.09	[a] 55.17 ± 0.45	56.10 ± 1.50

59.4 MPa at 1 K·min^{-1}); however, the observed differences are within experimental uncertainty. The corresponding thermograms are presented in Fig. 6.

Fig. 7 shows that the water content affects the breadth of the hydrate dissociation curve. However, the onset temperatures from both experiments are similar, as shown in Table 3. The water content does not affect the thermodynamic equilibrium but affects the water-to-hydrate conversion profile, as can be seen in Fig. 8, in which two samples are compared. The fraction of water converted to hydrate in the first run is significantly higher for the sample containing a larger amount of water (56.5 mg). This sample reached 95% water conversion in 12 cycles, while the sample containing 41.6 mg of water took 15 cycles for the same conversion. These findings indicate that a higher amount of water inside the cell favors hydrate formation, in accordance with previous work [46]. The droplet size can cause water to spread over a larger surface area on the cell, and it is crucial for hydrate formation. The hydrate formation was reported to be first limited by the clathrate reaction at the crystal-growing interface and not by the gas diffusion to said interface [40]. The second hydrate formation stage is under a diffusion-limited growth regime, thus the conversion of water to hydrate occurs at a similar rate in both cases after cycle 1, as seen in Fig. 8. However, the overall conversion (after 17 cycles) is the same for both runs.

The effect of pressure on the conversion of water to hydrate was evaluated by comparing experiments with the same water content. Fig. 9 refers to samples containing 56.5 mg of liquid water. The conversion profiles present two distinct stages: in each cycle, the conversion rate is higher up to about 90%, and lower after this threshold. As pressure increases, the conversion of water to hydrate tends to be larger and faster. This may be related to the higher methane solubility and diffusivity in water at higher pressures. The slight discrepancy observed at 31.5 MPa reminds the stochastic nature of hydrate formation – the lower conversion in the first cycle shifts the whole conversion curve.

3.1.2. *Enthalpy of dissociation and hydration number*

Although the standard method is accurate for determining dissociation temperatures, only the multicycle procedure provides accurate results for dissociation enthalpy by direct integration of thermograms, as explained in detail in section 2.4. Table 4 presents dissociation enthalpy values obtained from multicycle experiments data. Results estimated from pressure and temperature data previously obtained through standard experiments [46] are also included for comparison. The hydration number (n) was calculated based either on the fractional cages occupancies obtained by CSMGem predictions or on the iterative method. CSMGem presents hydration numbers slightly lower than those obtained by the iterative method. The cage occupancy increases due to the thermal expansivity effect on the hydrate lattice. However, the increase in compressibility factor caused by the increase in pressure may lead to a distortion in the lattice, which results in some empty cavities, since the molecules may not fit on them. It occurs mainly for systems containing larger guest molecules, such as ethane and CO_2. In the iterative method, the hydrate volume was estimated by considering the effect of temperature-dependent expansivity and isothermal compressibility factors on the lattice parameter. These factors affect the hydration number and hence the enthalpy of dissociation. The experimental enthalpy change used as a reference in the iterative method was 54.19 kJ/mol C_2H_6, as reported by Handa [28]. The lower differences between enthalpies obtained by the Clapeyron equation and by integration indicate that the iterative method provides the most reliable results, mainly at higher pressures. The multicycle method results are also compared with the average enthalpy value obtained from the integration performed in the standard procedure thermograms. Considering the presence of ice in such standard thermograms, the multicycle method shows to be the most appropriate one for determining the enthalpy due to the higher accuracy obtained during the integration of curves and the mitigation of the uncertainty related to extrapolated enthalpy for ice at high pressures.

Fig. 10 shows the enthalpies of dissociation obtained through the Clapeyron equation (A) and through the integration of dissociation curves from multicycle thermograms (B). Enthalpies obtained by the integration method are slightly higher than those obtained by the Clapeyron equation. The uncertainty of enthalpies calculated from Clapeyron method lies mainly on the determination of dP/dT and on the

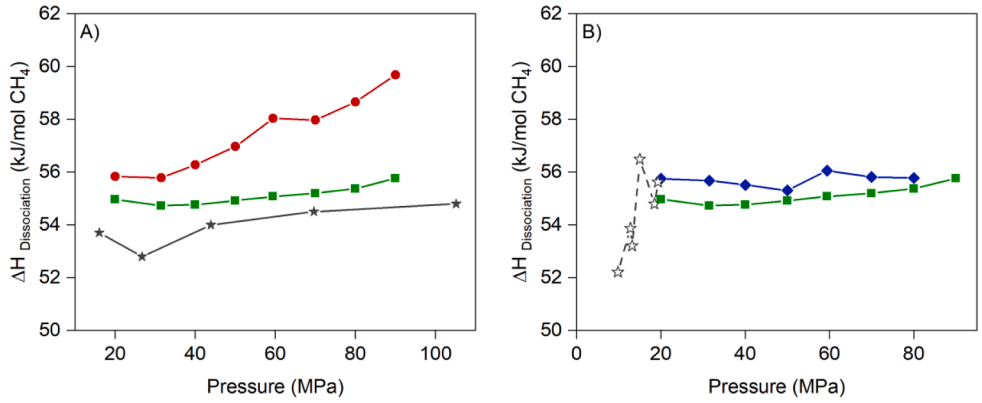

Fig. 10. Enthalpies of CH_4 hydrate dissociation determined by the Clapeyron equation (A) and the integration of dissociation curves (B) by the multicycle method: (●) *n* based on fractional cages occupancy; (■) *n* based on the iterative method; (★) Anderson [2]; (◆) Integration – *n* based on the iterative method (☆) Gupta [21].

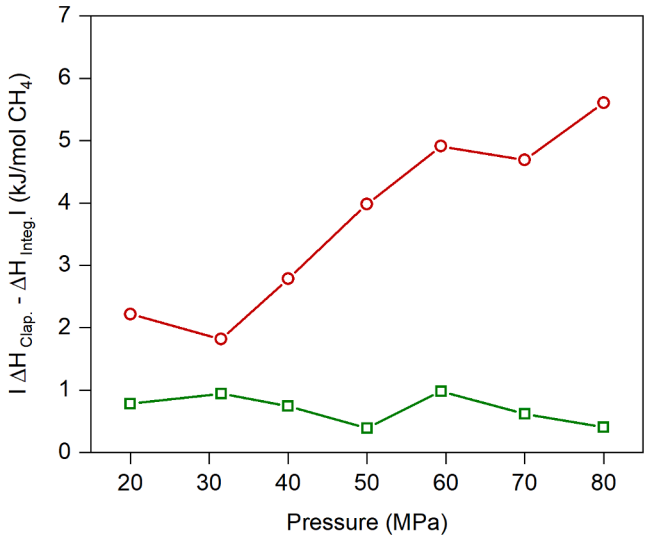

Fig. 11. Absolute differences between enthalpies of CH_4 hydrate dissociation obtained by the Clapeyron equation and the integration of dissociation curves by the multicycle method: (●) *n* based on fractional cages occupancy; (■) *n* based on the iterative method.

calculation of the hydrate volume. This highlights the importance of choosing an adequate equation to fit the experimental data. The integration can also be affected by the baseline determination, which is subject to experimental uncertainty. The enthalpies calculated using *n* based on fractional cages occupancy are highly dependent on the pressure, as shown in Fig. 11, which may indicate a limitation of this method.

Table 5 summarizes enthalpies of methane hydrates obtained in this work by using the multicycle method and found in the literature. No experimental values of enthalpies were found at similar conditions to this work. The main hydration number data from the literature are included. However, as pointed out in previous work [28], direct comparison is not strictly valid and a substantial deviation of hydration number can be found in the literature even for similar thermodynamic conditions.

The results obtained from iterations are more consistent and comparable to the data reported by Anderson [2]. To the best of our knowledge, the only experimental enthalpy data for methane hydrates obtained by the direct integration of thermograms at such high pressures were presented by Gupta [21]. However, these data were obtained using the standard method at lower pressures, which results in higher deviations. The great advantage of the multicycle method is the accuracy of the integration, due to the lower amount of ice and to the absence of recrystallization. The direct integration of the hydrate dissociation peak provides a more representative value of the total heat absorbed during hydrate dissociation.

Table 5
Enthalpies of CH_4 hydrates obtained in this work and found in literature.

Reference	Method	T (K)	ΔH (kJ/mol CH_4)	n
This work	HP-μDSC (multicycles)	291.74–304.33	55.70 ± 0.18	6.11 ± 0.02
	Clapeyron (multicycles)[a]		55.10 ± 0.24	
Menezes et al. [45]	Clapeyron (standard)[a]	291.74–305.48	55.17 ± 0.45	6.10 ± 0.09
Handa [23]	Calorimeter	273.15	54.19 ± 0.28	6.00 ± 0.01
Tsimpanogiannis et al. [67]	Clapeyron (MD)[b]	274–304	54.5 ± 1.5	Variable
Sun et al. [65]	Clausius-Clapeyron	284.4–289.5	59.1	–
Nasir et al. [54]	Clausius-Clapeyron	Q_1[c]	55.26	–
Kerkar et al. [35]	Clausius-Clapeyron	–	54.5–57.79	–
Gupta [21]	Clapeyron	290	53.86	
		298	53.98	6.0
		306	54.89	
Gupta [21]	Calorimeter (standard method)	280.60	54.90	6.0
		285.65	52.21	
		288.15	53.87	
		288.45	53.20	
		289.85	56.48	
		291.65	54.79	
		292.16	55.62	
Anderson [2]	Clapeyron	Q_1[c]	52.9	5.9 ± 0.3
		286	55.7	
		298	54	
		302	54.50	
		306	54.8	
Yoon et al. [71]	Clausius-Clapeyron	273.15	53.81	6.07

[a]Iterative method considering the enthalpy obtained by Handa [23] as reference.
[b]MD: Molecular dynamic simulations.
[c]Q1: Quadruple point (272.9 K; 2.563 MPa).

3.2. Ethane-Water system

3.2.1. Equilibrium data of C_2H_6 hydrates

Multiple cycles were also performed for ethane hydrate-forming

Table 6
Dissociation data of C_2H_6 hydrates obtained by HP-μDSC* using standard and multicycle methods.

P (MPa)	n° Cycles	Ø (K·min^{-1})	H_2O (mg)	H_2O Conv. (%)	T $_{ONSET}$ (K)	T $_{PEAK}$ (K)	T $_{ENDSET}$ (K)
5	1	1.0	53.3	–	287.96	288.65	290.01
	38	0.2	53.3	97.53	288.35	289.11	291.26
9.8	1	1.0	42.3	–	288.71	289.62	291.29
	32	0.2	42.3	98.67	289.00	289.59	291.74
20	1	1.0	53.3	–	290.27	290.83	292.24
	42	0.2	53.9	99.80	290.61	291.29	293.18
50	1	1.0	53.3	–	293.93	294.60	296.09
	41	0.2	51.9	99.07	294.49	294.92	296.91

* – Standard uncertainties are u(T) = 0.3 K, u(x) ≈ 0.0002 and u(P) = 0.1 MPa.

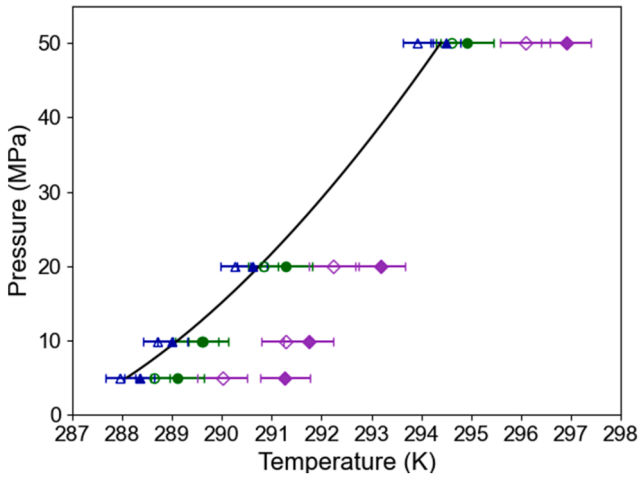

Fig. 12. Dissociation data of C_2H_6 hydrates obtained by HP-μDSC using standard method (empty symbols) and multicycles method (full symbols): (▲) onset temperature; (●) peak temperature; (◆) endset temperature. Black lines refer to CSMGem predictions.

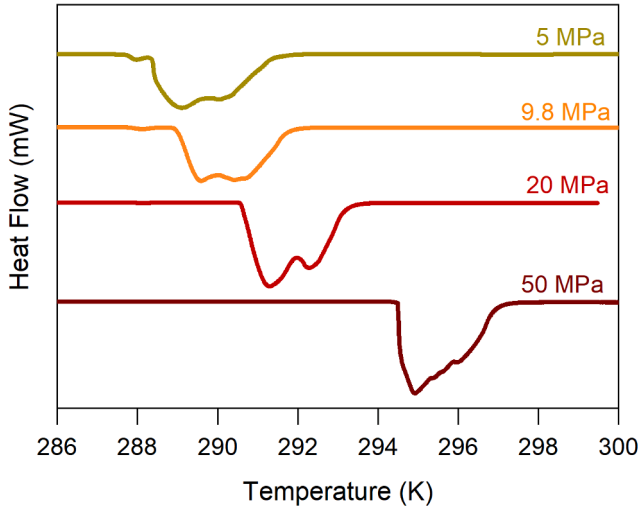

Fig. 13. Thermograms of C_2H_6 hydrates dissociation obtained by the multicycle method.

systems at 5, 9.8, 20, and 50 MPa. The results are shown in Table 6 and compared to data obtained by the standard method in Fig. 12. Onset temperatures are in good agreement. However, the differences among

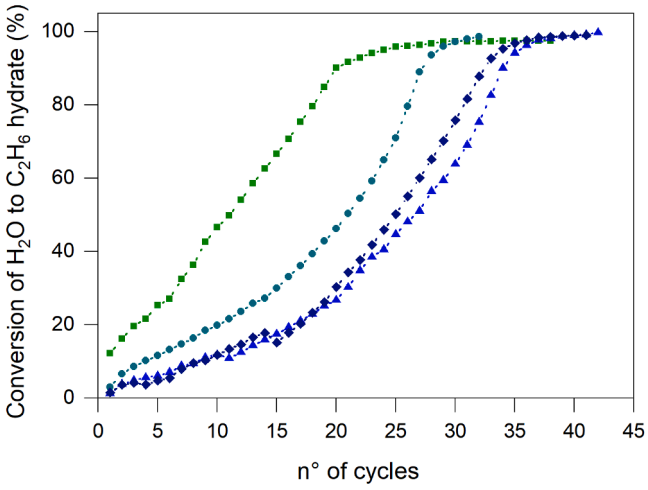

Fig. 14. Conversion of water to C_2H_6 hydrate throughout multicycles at different pressures: (■) 5 MPa – 53.3 mg H_2O (●) 9.8 MPa – 42.3 mg H_2O (▲) 20 MPa – 53.9 mg H_2O (◆) 50 MPa – 51.9 mg H_2O.

Table 7
Enthalpies of C_2H_6 hydrates based on experimental data obtained by HP-μDSC* applying the multicycle method at 0.2 K·min^{-1}.

Hydration number (*n*) based on predictions of fractional cages occupancy				
P (MPa)	T (K)	*n*	△H $_{Clapeyron.}$ (kJ/mol C_2H_6)	△H $_{Integration}$ (kJ/mol C_2H_6)
5	288.35	7.74	74.79	57.00
9.8	289.00	7.72	67.35	64.85
20	290.61	7.68	62.20	65.51
50	294.49	7.59	55.76	71.89
Average ± $CI_{95\%}$		7.68 ± 0.06	65.02 ± 7.89	64.81 ± 5.98
Hydration number (*n*) from Iterative Method				
P (MPa)	T (K)	*n*	△H $_{Clapeyron.}$ (kJ/mol C_2H_6)	△H $_{Integration}$ (kJ/mol C_2H_6)
5	288.35	8.69	66.41	64.00
9.8	289.00	7.95	65.31	66.70
20	290.61	7.44	64.72	63.45
50	294.49	6.92	64.46	65.53
Average ± $CI_{95\%}$		7.75 ± 0.74	65.23 ± 0.85	64.92 ± 1.45

* – Standard uncertainties are u(T) = 0.3 K, u(x) ≈ 0.0002 and u(P) = 0.1 MPa.

peak and endset temperatures are higher, which is due to the amount of hydrate formed, considerably larger for the multicycle analyses.

Fig. 13 shows that the hydrate dissociation curves obtained through

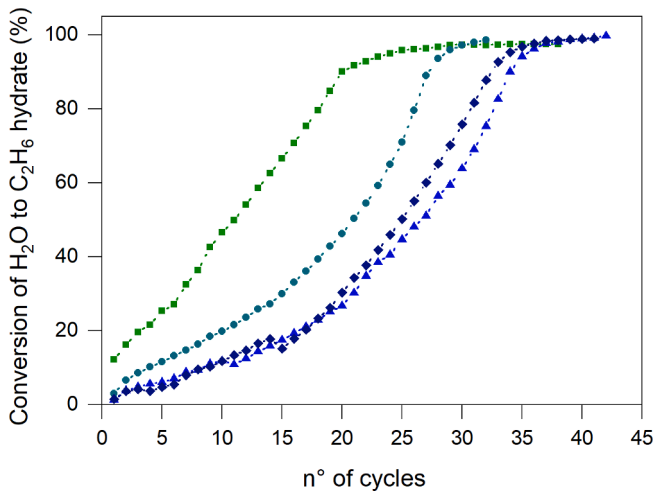

Fig. 15. (A) Enthalpies of C_2H_6 hydrate dissociation: (●) Clapeyron equation – *n* based on fractional cages occupancy; (■) Clapeyron equation – *n* based on the iterative method; (◆) Integration – *n* based on the iterative method. (B) Absolute deviations between enthalpies of C_2H_6 hydrate dissociation obtained by the Clapeyron equation and the integration of dissociation curves: (●) *n* based on fractional cages occupancy; (■) *n* based on the iterative method.

Table 8
Enthalpies of C_2H_6 hydrates obtained in this work and found in the literature.

Reference	Method	T (K)	ΔH (kJ/mol C_2H_6)	n
This work	HP-μDSC (multicycles)	288.35–294.49	64.92 ± 1.45	7.75 ± 0.74
	Clapeyron (multicycles)[a]		65.23 ± 0.85	
Menezes et al. [45]	Clapeyron (standard)[a]	287.96–296.00	65.01 ± 0.22	7.52 ± 0.24
Nakagawa et al. [53]	Calorimeter	283.00–286.00	71.10	–
Yoon et al. [71]	Clausius-Clapeyron	273.15	71.34	7.77
Handa [23]	Calorimeter	273.15	71.80	7.67 ± 0.02

[a] Iterative method considering the enthalpy obtained by Handa [28] as reference.

Table 9
Dissociation data of CO_2 hydrates obtained by HP-μDSC* using standard and multicycle methods, both at 1 K·min^{-1}.

P (MPa)	n° Cycles	H_2O (mg)	H_2O Conv. (%)	T ONSET (K)	T PEAK (K)	T ENDSET (K)
9.8	1	48.9	–	283.70	285.41	286.88
	25	48.9	99.67	283.52	286.17	289.88
20	1	48.9	–	284.87	286.72	288.70
	24	48.9	99.93	284.42	288.27	290.91
40	1	53.4	–	286.15	287.99	289.53
	21	53.4	~100	286.15	289.64	292.63
50	1	48.9	–	286.74	288.17	289.66
	‘7	53.4	~100	286.61	289.03	292.75

* – Standard uncertainties are u(T) = 0.3 K, u(x) ≈ 0.0002 and u(P) = 0.1 MPa.

the multicycle method present distinct overlapping peaks, which may indicate the presence of hydrate layers with different occupancy degrees, as the hydrate formation is limited by the gas diffusion into the solid phase.

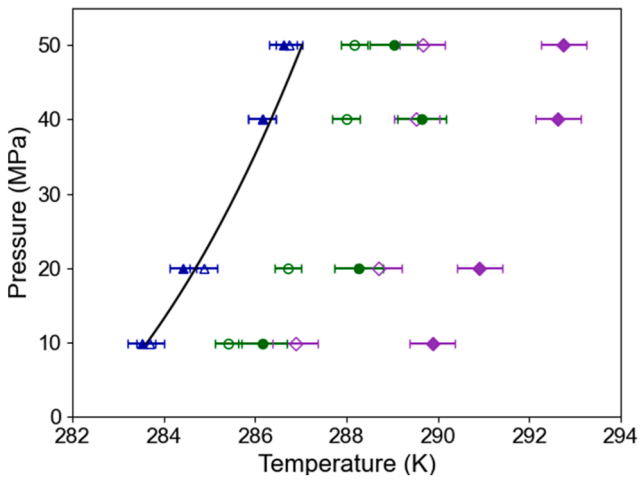

Fig. 16. Dissociation data of CO_2 hydrates obtained by HP-μDSC using standard method (empty symbols) and multicycles method (full symbols): (▲) onset temperature; (●) peak temperature; (◆) endset temperature. Black lines refer to CSMGem predictions.

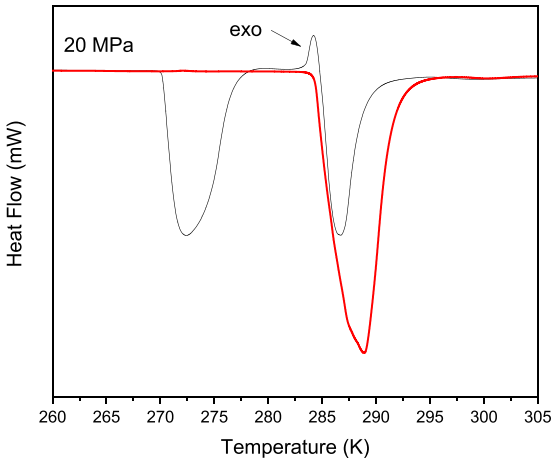

Fig. 17. Heating thermograms of carbon dioxide hydrate obtained by the standard DSC method (▬) and the multicycle method (▬). Samples were analyzed at 20 MPa using a cooling and a heating rate of 1 K·min^{-1}.

A main difference from the methane hydrate results concerns the water conversion rate. Methane hydrates required less than 16 cycles for 90% of water conversion (Fig. 9) for a minimum pressure of 9.8 MPa, whereas Fig. 14 shows that ethane-water systems required at least 20 cycles to reach the same conversion. The larger molecular size of ethane and its lower diffusivity in water, compared to methane, may hinder its incorporation into the cavities, therefore requiring a larger number of cycles.

3.2.2. Enthalpy of dissociation and hydration number

Table 7 presents the enthalpies of dissociation obtained for ethane hydrates by the Clapeyron and integration methods. The results are based only on multicycle analyses, since the standard ones were inadequate in this case to determine the enthalpy of dissociation, as the higher amount of ice formed made the integration process inaccurate. The calculated hydration number was higher when applying the iterative method. Fig. 15 shows that the hydration number based on

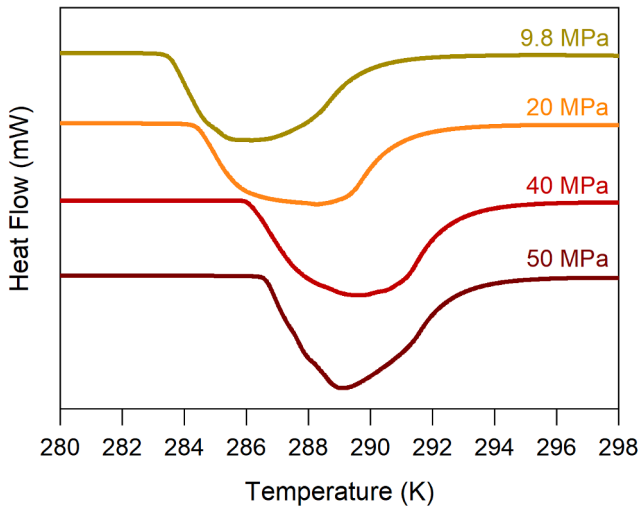

Fig. 18. Thermograms of CO_2 hydrates dissociation obtained by the multicycle method.

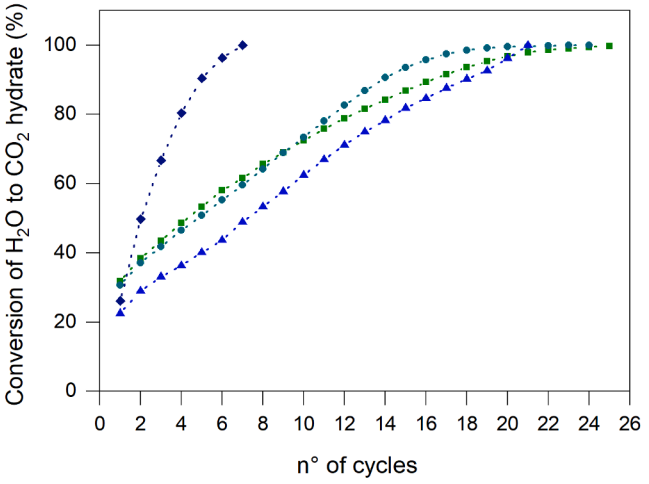

Fig. 19. Conversion of water to CO_2 hydrate throughout multicycles at different pressures: (■) 9.8 MPa – 48.9 mg H_2O (●) 20 MPa – 48.9 mg H_2O (▲) 40 MPa – 53.4 mg H_2O (◆) 50 MPa – 53.4 mg H_2O.

CSMGem predictions does not provide consistent results. A better agreement is found between enthalpies from the Clapeyron equation and integration when applying the iterative method. The average deviations and the respective confidence intervals (95%), shown in Table 7, indicate that the iterative method is more reliable. The enthalpy used as a reference was 71.8 kJ/ mol C_2H_6, as reported by Handa [28].

Table 8 presents a comparison of values obtained in this work and from the literature. No experimental values of enthalpy were found in the literature at similar conditions, as the analyses presented herein were performed above the upper quadruple point (Q_2), which connects L_W-H-L_{HC} and L_W-H-V_{HC} equilibrium lines. The calculated enthalpy changes are slightly lower than those obtained from the literature (below Q_2) since the hydrate dissociation delivers ethane in form of compressed liquid instead of vapor. The latent heat of ethane vaporization is about 5 kJ/mol [18], which is close to the difference between the enthalpies obtained in this work (above Q_2) and found in the literature (below Q_2).

Table 10
Enthalpies of CO_2 hydrates based on experimental data obtained by HP-μDSC* applying the multicycle method.

Hydration number (n) based on predictions of fractional cage occupancy				
P (MPa)	T (K)	n	$\triangle H_{Clapeyron.}$ (kJ/mol CO_2)	$\triangle H_{Integration}$ (kJ/mol CO_2)
9.8	283.52	6.3	52.58	47.05
20	284.42	6.2	51.44	46.62
40	286.15	6.1	53.38	45.92
50	286.61	6.0	52.27	46.08
Average ± $CI_{95\%}$		6.15 ± 0.11	52.42 ± 0.79	46.42 ± 0.51
Hydration number (n) from Iterative Method (ΔH^a)				
P (MPa)	T (K)	n	$\triangle H_{Clapeyron.}$ (kJ/mol CO_2)	$\triangle H_{Integration}$ (kJ/mol CO_2)
9.8	283.52	6.2	54.17	46.16
20	284.42	6.1	53.82	45.49
40	286.15	6.1	53.65	45.84
50	286.61	6.0	53.50	45.70
Average ± $CI_{95\%}$		6.07 ± 0.08	53.79 ± 0.28	45.80 ± 0.28
Hydration number (n) from Iterative Method (ΔH^b)				
P (MPa)	T (K)	n	$\triangle H_{Clapeyron.}$ (kJ/mol CO_2)	$\triangle H_{Integration}$ (kJ/mol CO_2)
9.8	283.52	6.6	47.97	49.67
20	284.42	6.5	47.72	48.50
40	286.15	6.4	47.57	48.18
50	286.61	6.3	47.48	47.84
Average ± $CI_{95\%}$		6.43 ± 0.16	47.69 ± 0.21	48.55 ± 0.78

* – Standard uncertainties are u(T) = 0.3 K, u(x) ≈ 0.0002 and u(P) = 0.1 MPa.
[a] Iterations considering ΔH obtained by Kang et al. [31] as reference.
[b] Iterations considering ΔH obtained by Anderson [1] as reference.

3.3. Carbon Dioxide-Water system

3.3.1. Equilibrium data of CO_2 hydrates

Table 9 and Fig. 16 present the dissociation temperatures obtained for carbon dioxide hydrates at different pressures. Since carbon dioxide at critical conditions is deleterious for the elastomer seal inside the pressure gauge, shorter analyses were carried out and the cooling/heating rate applied for this system was kept at 1 K·min^{-1}. As previously shown, the influence of the rate on onset temperatures and enthalpy is almost negligible. The overall behavior of the dissociation curves (amount of hydrate formed and wider dissociation peaks) is similar to those previously observed for multiple cycles when compared to the standard procedure.

Fig. 17 shows heating thermograms of carbon dioxide hydrate obtained in this work by the standard DSC method and the multicycle method. No exothermic peak related to metastable phases is observed when the multicycle method is applied. The onset temperatures for the multicycle analysis are remarkably close to those obtained by the standard analysis. While onset temperatures tend to be slightly lower for the multicycle method, deviations are within experimental uncertainty.

Thermograms of CO_2 hydrate dissociation obtained by the multicycle method are shown in Fig. 18. They seem to be smoother than methane and ethane thermograms (Figs. 6 and 13, respectively). This can be explained by the fact that multicycle analyses of CO_2 hydrate were run at higher heating rate than for methane and ethane hydrates, which enlarge the dissociation curves. Thus, distinct peaks are not so evident as

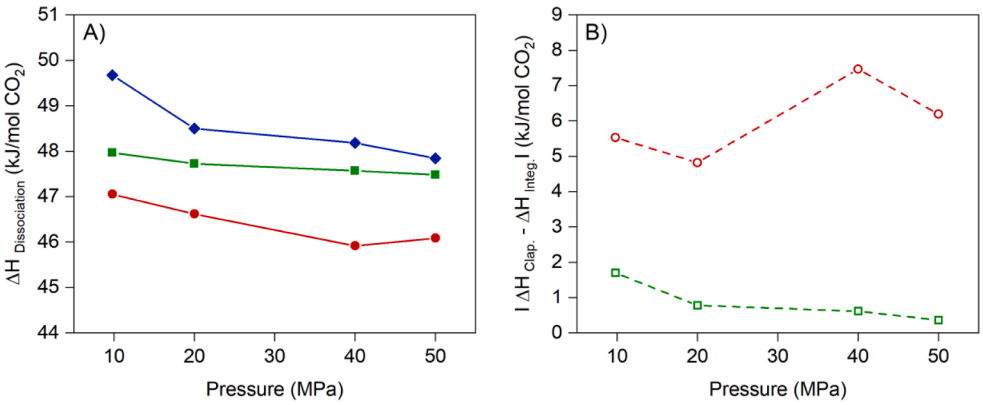

Fig. 20. (A) Enthalpies of CO_2 hydrate dissociation: (●) Clapeyron equation – *n* based on fractional cages occupancy; (■) Clapeyron equation – *n* based on the iterative method; (◆) Integration – *n* based on the iterative method. (B) Absolute deviations between enthalpies of CO_2 hydrate dissociation obtained by the Clapeyron equation and the integration of dissociation curves: (●) *n* based on fractional cages occupancy; (■) *n* based on the iterative method. All the data shown are referred to the enthalpy reported by Anderson [1] as reference.

Table 11
Enthalpies of CO_2 hydrates obtained in this work and found in the literature.

Reference	Method	T (K)	ΔH (kJ/mol CO_2)	n
This work	HP-μDSC (multicycles)	283.52–286.61	48.55 ± 0.78	6.43 ± 0.16
	Clapeyron (multicycles)[a]		47.69 ± 0.21	
Menezes et al. [46]	Clapeyron (standard)[a]	283.70–288.45	47.55 ± 0.15	6.42 ± 0.09
Nasir et al. [54]	Clausius-Clapeyron	Q_1	53.29	–
Sabil [57]	Clausius-Clapeyron	273.15–282.06	75.37–56.85	–
Yoon et al. [71]	Clausius-Clapeyron	273.15	57.66	6.21
Anderson [1]	Clapeyron	271.8–283.1[b]	63.6–57.6[b]	5.7–6.4
Kang et al. [31]	Microcalorimeter	273.65	65.22	7.23
Bozzo et al. [5]	Clausius-Clapeyron	273.15	58.99	7.3 ± 0.1
Vlahakis et al. [70]	Clausius-Clapeyron	273.20	59.90	7.3

[a]Iterative method considering the enthalpy obtained by Anderson [1] as reference.
[b]Corresponding to Q_1 (1.256 MPa) and Q_2 (4.499 MPa)

they are for methane and ethane hydrates.

Finally, the water conversion over multiple cycles is shown in Fig. 19. Due to the solubility and diffusivity of CO_2, faster conversion rates were expected in this system compared to methane and ethane hydrates. This can effectively be observed at 50 MPa, since only 6 cycles were enough to reach more than 90% of water conversion. However, this is not observed for lower pressures, in which the water conversion required as many cycles as methane hydrate samples. This fact recalls that pressure and H_2O sample size affect the water conversion rate to hydrate, but the process has also a stochastic nature.

3.3.2. *Enthalpy of dissociation and hydration number*

The results of dissociation enthalpies for CO_2 hydrates are presented in Table 10 and Fig. 20. Two different enthalpies from the literature were used as reference to calculate the hydration number through the iterative method: i) calorimetric data at 273.65 K from Kang et al. [31]; ii) data from the Clapeyron equation calculated by Anderson [1] at the upper quadruple point (283.1 K and 4.45 MPa). A significant difference is observed. Anderson [1] also obtained a difference of about 5 kJ·mol^{-1} for the enthalpies calculated on the L_W-H-V_{HC} equilibrium lines and suggested that a systematic error may have occurred in the calorimetric measurements from Kang et al. [31]. The calorimetric results for methane hydrate reported by Kang et al. [31] also present a significant deviation from enthalpies obtained by Handa [28], who used a direct method.

The value of *n* tends to decrease as the pressure increases. The volumetric compressibility κ_T is found to be $3.0{\cdot}10^{-4}$, $3.0{\cdot}10^{-7}$ and $3.0{\cdot}10^{-5}$ for methane, ethane and carbon dioxide, respectively [4]. Therefore, the effect of the compressibility factor on the lattice parameter is lower for ethane and carbon dioxide hydrates, and the effect of thermal expansivity prevails and favors the cage occupancy, decreasing the hydration number.

Fig. 20 shows the dissociation enthalpies (A) and absolute differences from results obtained by Clapeyron equation and integration method (B). The average deviations and the respective confidence intervals (95%) shown in Table 10 indicate that using the enthalpy reference from Anderson [1] provides the most reliable results, as the results using either the integration method or the Clapeyron equation are similar (Fig. 20B). No data were found in the literature for CO_2 hydrate dissociation above Q_2; for data below Q_2, previously reported results vary in a broad temperature range, as listed in Table 11. The latent heat of CO_2 vaporization is around 9 kJ/mol (NIST Webbook), which explains the difference of the enthalpy change determined in this work to those from the literature.

4. Conclusions

This work presents new experimental data for the dissociation enthalpy of methane, ethane and carbon dioxide hydrates at high pressures, using the multicycle method and numerical iterations for determining the hydration number. The results show that the multicycle method increases the water (ice) conversion to hydrate. This conversion depends on the guest molecule: for ethane, a larger molecule than methane and carbon dioxide, more cycles are necessary to reach 90% of water conversion to hydrate, whereas the fraction of hydrate formed in the first cycle is much higher for carbon dioxide than for methane and ethane hydrates, due to the higher solubility and diffusivity of CO_2 in water. The dissociation onset temperatures obtained by the multicycle

method are accurate, close to those provided by the standard method, which is reliable for this determination. Finally, in contrast to the standard method, the multicycle method allows the accurate determination of the hydrate dissociation enthalpy regardless of the guest molecule used to form the hydrate, since no free water or ice is practically present in the system. The absence of a recrystallization process and the higher conversion of water into hydrate also reduces the uncertainty during the baseline drawing to integrate the thermograms.

CRediT authorship contribution statement

María Dolores Robustillo: Conceptualization, Methodology, Data curation, Investigation, Formal analysis, Validation, Resources, Writing – original draft, Writing – review & editing, Supervision, Project administration, Funding acquisition. **Davi Eber Sanches de Menezes:** Conceptualization, Methodology, Data curation, Investigation, Formal analysis, Writing – original draft, Writing – review & editing. **Pedro de Alcântara Pessôa Filho:** Formal analysis, Validation, Writing – review & editing.

Declaration of Competing Interest

The authors declare that they have no known competing financial interests or personal relationships that could have appeared to influence the work reported in this paper.

Acknowledgments

The authors thank the financial support of FAPESP (processes 2014/02140-7, 2014/25740-0 and 2015/23148-9) and CNPq (processes 132505/2015 and 306184/2017-6). The help of members of the laboratory GenBio (USP) is also gratefully acknowledged.

Appendix A Fitting of Experimental Data to Polynomial Equations

The factor dP/dT is required to apply the Clapeyron equation for determining the enthalpy of dissociation. Thus, the experimental data (temperature and pressure) obtained by HP-μDSC were fitted to convenient equations for each system, as presented in Table A.1. Then, the respective equation was derived to obtain the factor dP/dT.

$$\Delta H = \frac{dP}{dT} \cdot T \cdot \Delta V \tag{A.1}$$

Table A1
Empirical equations and coefficients fitted to the experimental data obtained by the multicycle method via HP-μDSC.

Hydrate	Equation	Coefficients	
CH_4	$y = a + b{\cdot}x + c{\cdot}x{\cdot}\ln(x) + \frac{d{\cdot}x}{\ln(x)} + \frac{e}{x^{1.5}}$	a	$-6.00{\cdot}10^{5}$
		b	$-3.55{\cdot}10^{9}$
		c	$-3.98{\cdot}10^{8}$
		d	$-8.27{\cdot}10^{9}$
		e	9.31
C_2H_6	$y = a + \frac{b}{x^{0.5}} + c{\cdot}\frac{\ln(x)}{x^{2}}$	a	$-2.93{\cdot}10^{5}$
		b	$4.30{\cdot}10^{4}$
		c	$2.55{\cdot}10^{6}$
CO_2	$y = a + b{\cdot}x^{0.5} + \frac{c}{\ln(x)}$	a	$-8.71{\cdot}10^{5}$
		b	$-7.22{\cdot}10^{8}$
		c	$2.00{\cdot}10^{11}$
		d	$-1.84{\cdot}10^{13}$

Appendix B Molar Volume of the Hydrate Unit Cell

The molar volume of the hydrate unit cell (V_{uc}), required to calculate the volume of hydrate containing one mole of hydrocarbon or CO_2 (V_{hyd}), was determined according to the equation below, detailed in previous work [46]:

$$V_{uc}(T,P,x) = V_{uc_0} \bullet \exp\left[\alpha_{v1} \bullet (T - T_0) + \frac{\alpha_{v2}}{2} \bullet (T - T_0)^2 + \frac{\alpha_{v3}}{3} \bullet (T - T_0)^3 - \kappa_{T(v)} \bullet (P - P_0)\right]$$

The reference temperature (T_0), the reference lattice parameter (a_0) used to calculate V_{uc_0}, and the compressibility coefficient (κ_T) obtained from the literature are presented in Table A.2. The lattice parameter (a) found for each temperature and its corresponding pressure are presented in Fig. B1 for methane, ethane, and carbon dioxide hydrates. The lattice parameter is calculated by the linear version of the equation above [30]. The unit cell volume corresponds to the cubic values of the lattice parameter.

Table A2
Reference parameters from the literature for estimating the molar volume of the hydrate unit cell.

Hydrate	Methane	Ethane	CO_2
Reference Temperature (T_0)/K	271 [a]	217[b]	173[c]
Lattice parameter (a_0)/Å	11.960 [a]	11.995[b]	11.893[c]
Compressibility Coefficient (κ_T)/MPa^{-1}	3.10^{-4} [d]	3. 10^{-7} [d]	3. 10^{-5} [d]

[a] Klapproth et al. [38],[b] Hester et al. [30],[c] Udachin et al. [68]; [d] Ballard [4].

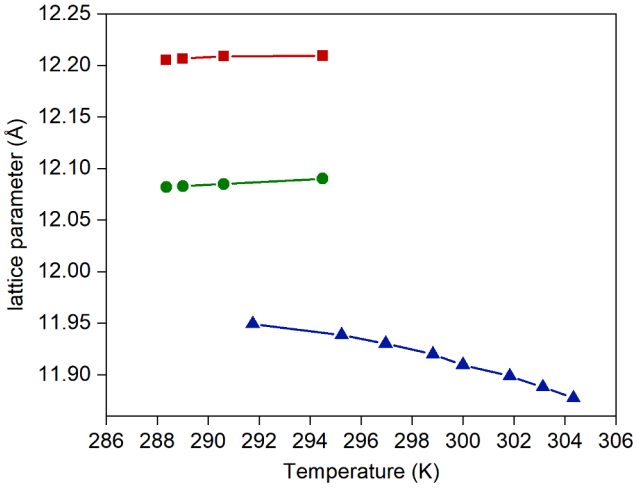

Fig. B1. Lattice parameter calculated considering the experimental data by the multicycle method and the thermal expansivity and compressibility coefficients obtained by correlations with literature data: (▲) methane hydrate; (●) ethane hydrate; (■) carbon dioxide hydrate.

References

[1] Anderson GK. Enthalpy of dissociation and hydration number of carbon dioxide hydrate from the Clapeyron equation. J Chem Thermodyn 2003;35:1171–83.
[2] Anderson GK. Enthalpy of dissociation and hydration number of methane hydrate from the Clapeyron equation. J Chem Thermodyn 2004;36:1119–27.
[3] Babu P, Nambiar A, He T, Karimi IA, Lee JD, Englezos P, et al. A review of clathrate hydrate based desalination to strengthen energy–water nexus. ACS Sustain Chem Eng 2018;6:8093–107.
[4] Ballard, A.L. A non-ideal hydrate solid solution model for a multi-phase equilibria program. Ph.D. Thesis, Colorado School of Mines, 2001.
[5] Bozzo AT, Chen H-S, Kass JR, Barduhn AJ. The proprieties of Hydrate of chlorine and carbon dioxide. Desalination 1975;16:303–20.
[6] BRIDGMAN, P.W. Water, in the liquid and five solid forms, under pressure. Proceedings of the American Academy of Arts and Sciences XLVII, v. 13, p. 439-558, 1912.
[7] CHAZALLON, B.; NOBLE, J. A.; DESMEDT, A. Spectroscopy of Gas Hydrates: From Fundamental Aspects to Chemical Engineering, Geophysical and Astrophysical Applications. Chapter 2 in Gas Hydrates 1: Fundamentals, Characterization and Modeling, First Edition. Edited by Daniel Broseta, Livio Ruffine and Arnaud Desmedt. © ISTE Ltd 2017. Published by ISTE Ltd and John Wiley & Sons, Inc.
[8] Circone S, Kirby SH, Stern LA. Thermodynamic calculations in the system CH4-H2O and methane hydrate phase equilibria. J Phys Chem B 2006;110:8232–9.
[9] Dalmazzone D, Clausse D, Dalmazzone C, Herzhaft B. The stability of methane hydrates in highly concentrated electrolyte solutions by differential scanning calorimetry and theoretical computation. Am Mineral 2004;89:1183–91.
[10] DALMAZZONE, D.; SALES SILVA, L. P.; DELAHAYE, A.; FOURNAISON, L Calorimetric Characterization of Clathrate and Semiclathrate Hydrates. Chapter 4 in Gas Hydrates 1: Fundamentals, Characterization and Modeling, First Edition. Edited by Daniel Broseta, Livio Ruffine and Arnaud Desmedt. © ISTE Ltd 2017. Published by ISTE Ltd and John Wiley & Sons, Inc.
[11] De Forcrand R. Comptes Rendus 1902;135:959–61.
[12] Delahaye A, Fournaison L, Marinhas S, Chatti I, Petitet JP, Dalmazzone D, Fürst W. Effect of THF on equilibrium pressure and dissociation enthalpy of CO2 hydrates applied to secondary refrigeration. Ind Eng Chem Res 2006;45:391–7.
[13] DELAHAYE, A. FOURNAISON, L.; DALMAZZONE, D. Use of Hydrates for Cold Storage and Distribution in Refrigeration and Air-Conditioning Applications. Chapter 15 in Gas Hydrates 2: Geoscience Issues and Potential Industrial Applications. Edited by Livio Ruffine, Daniel Broseta and Arnaud Desmedt. 2018.
[14] DENYS, S.; SCHLÜTER, O.; HENDRICKX, M.E.G.; KNORR, D. Effects of High Pressure on Water-Ice Transitions in Foods. In: Hendrickx M.E.G., Knorr D., Ludikhuyze L., Van Loey A., Heinz V. (eds) Ultra High Pressure Treatments of Foods, chapter 8, p. 242. Food Engineering Series. Springer, Boston, MA, 2001.
[15] Deschamps J, Dalmazzone D. Dissociation enthalpies and phase equilibrium for TBAB semi–clathrate hydrates of N2, CO2, N2 + CO2 and CH4 + CO2. J Therm Anal Calorim 2009;98:113–8.
[16] Deschamps J, Dalmazzone D. Hydrogen storage in semiclathrate hydrates of tetrabutyl ammonium chloride and tetrabutyl phosphonium bromide. J Chem Eng Data 2010;9:3395–9.
[17] Diamond, L.W.; Akinfiev, N.N. Solubility of CO2 in water from −1.5 to 100 ∘C and from 0.1 to 100 MPa: evaluation of literature data and thermodynamic modelling. Fluid Phase Equilibria, v. 208, p. 265-290, 2003.
[18] Friend DG, Ingham H, Fly JF. Thermophysical properties of ethane. J Phys Chem Ref Data 1991;20:275.
[19] Fukumoto A, Dalmazzone D, Paricaud P, et al. Experimental measurements and modeling of the dissociation conditions of tetrabutylammonium chloride semiclathrate hydrates in the presence of hydrogen. J Chem Eng Data 2015;60:343–50.
[20] Fukusako S. Thermophysical properties of ice, snow, and sea ice. Int J Thermophys 1990;11:353–72.
[21] Gupta, A. Methane Hydrate Dissociation Measurements and Modeling: The Role of Heat Transfer and Reaction Kinetic, Ph.D. thesis, Colorado School of Mines, Golden, Colorado, USA, 2007.
[22] Gupta A, Lachance J, Sloan ED, Koh CA. Measurements of methane hydrate heat of dissociation using high pressure differential scanning calorimetry. Chem Eng Sci 2008;63:5848–53.
[23] Handa YP. Calorimetric determinations of the compositions, enthalpies of dissociation, and heat capacities in the range 85 to 270 K for clathrate hydrates of xenon and krypton. J Chem Thermodyn 1986;18:891–902.
[24] Handa YP. Compositions enthalpies of dissociation, and heat capacities in the range 85 to 270 K for clathrate hydrates of methane, ethane, and propane, and enthalpy of dissociation of isobutane hydrate as determined by heat-flow calorimeter. J Chem Thermodyn 1986;18:915.
[25] Handa YP. A calorimetric study of naturally occurring gas. Ind Eng Chem Res 1988;27:872–4.
[26] Handa YP, Hawkins RE, Murray JJ. Calibration and testing of a Tian– Calvet heat-flow calorimeter. Enthalpies of fusion and heat capacities for ice and tetrahydrofuran hydrate in the range 85 to 270 K. J Chem Thermodyn 1984;16:623–32.
[27] Handa YP, Yamamuro O, Oguni M, et al. Low temperature heat capacities of xenon and krypton clathrate hydrates. J Chem Thermodyn 1989;21:1249–62.
[28] Handa YP. Compositions, enthalpies of dissociation, and heat capacities in the range 85 to 270 K for clathrate hydrates of methane, ethane, and propane, and enthalpy of dissociation of isobutane hydrate, as determined by a heat-flow calorimeter. J Chem Thermodyn 1986;18:915–21.
[29] Hassanpouryouzband A, Joonaki E, Farahani MV, Takeya T, Ruppel C, Yang J, et al. Gas hydrates in sustainable chemistry. Chem Soc Rev 2020;49:5225–309.
[30] Hester KC, Huo Z, Ballard AL, Koh CA, Miller KT, Sloan ED. Thermal expansivity for sI and sII clathrate hydrates. J Phys Chem B 2007;111:8830–5.
[31] Kang S-P, Lee H, Ryu B-J. Enthalpies of dissociation of clathrate hydrates of carbon dioxide, nitrogen, (carbon dioxide + nitrogen), and (carbon dioxide + nitrogen + tetrahydrofuran). J Chem Thermodyn 2001;33:513–21.
[32] Kang KC, Linga P, Park K, Choi SJ, Lee JD. Seawater desalination by gas hydrate process and removal characteristics of dissolved ions (Na+, K+, Mg2+, Ca2+, B3+, Cl−, SO42−). Desalination 2014;353:84–90.
[33] Karimi A, Dolotko O, Dalmazzone D. Hydrate phase equilibria data and hydrogen storage capacity measurement of the system H2 + tetrabutylammonium hydroxide + H2O. Fluid Phase Equilib 2014;361:175–80.
[34] Karino S, Hane H, Makita I. Behavior of water and ice at low temperature and high pressure. In: Hayashi R, Kunugi S, Shimada S, Suzuki A, editors. High Pressure Bioscience. Kyoto: San-Ei Suppan; 1994. p. 2–9.
[35] Kerkar PB, Horvat K, Mahajan D, Jones KW. Formation and dissociation of methane hydrates from seawater in consolidated sand: mimicking methane hydrate dynamics beneath the seafloor. Energies 2013;6:6225–41.
[36] Kvenvolden KA. Gas hydrates—geological perspective and global change. Rev Geophys 1993;31(2):173–87.
[37] Kim S, Choi SD, Seo Y. CO2 capture from flue gas using clathrate formation in the presence of thermodynamic promoters. Energy 2017;118:950–6.
[38] Klapproth A, Goreshnik E, Staykova D, Klein H, Kuhs W. Structural studies of gas hydrates. Can J Phys 2003;81:503–18.
[39] Krichevsky IR, Karnovsky JS. Thermodynamical calculations of solubilities of nitrogen and hydrogen in water at high pressures. Am Chem Soc 1935;57:2168.
[40] Liang H, Guan D, Shi K, Yang L, Zhang L, Zhao J, et al. Characterizing mass-transfer mechanism during gas hydrate formation from water droplets. Chem Eng J 2022;428:132626.
[41] Lievois JS, Perkins R, Martin RJ, Kobayashi R. Development of an automated high pressure heat flux calorimeter and its application to measure the heat of dissociation and hydrate numbers of methane hydrate. Fluid Phase Equilib 1990;59:73–97.
[42] Marinhas S, Delahayea A, Fournaisona L, Dalmazzone D, Furst W, Petitet JP. Modelling of the available latent heat of a CO2 hydrate slurry in an experimental loop applied to secondary refrigeration. Chem Eng Process 2006;45:184–92.
[43] Martinez MC, Dalmazzone D, Fürst W, et al. Thermodynamic properties of THF + CO2 hydrates in relation with refrigeration applications. AIChE J 2008;54(4):1088–95.

[44] Mayoufi N, Dalmazzone D, Fürst W, Delahaye A. Fournaison. CO2 enclathration in hydrates of peralkyl-(ammonium/phosphonium) salts. J Chem Eng Data 2010;55:1271–5.
[45] Mendez ASJ, Muñoz-Iglesias V, Izquierdo-Ruíz F, Prieto-Ballesteros O. Salting-out phenomenon induced by the clathrate hydrates formation at high-pressure. J Phys Conf Series 2017;950:042042.
[46] Menezes DES, Pessoa filho PA, Robustillo MD. Phase equilibrium for methane, ethane and carbon dioxide hydrates at pressures up to 100 MPa through high-pressure microcalorimetry: experimental data, analysis and modeling. Fluid Phase Equilib 2020;518:112590.
[47] Menezes DES, Pessôa Filho PA, Robustillo MD. Use of 1-Butyl-3-methylimidazolium-based ionic liquids as methane hydrate inhibitors at high-pressure conditions. Chem Eng Sci 2020;212:115323.
[48] Menezes DES, Ralha TW, Franco LFM, Pessôa filho PA, Robustillo MD. Simulation and experimental study of methane-propane hydrate dissociation by high-pressure differential scanning calorimetry. Braz J Chem Eng 2018;35:403–14.
[49] Menezes DES, Sum AK, Desmedt A, Pessôa filho PA, Robustillo MD. Coexistence of sI and sII in methane-propane hydrate former systems at high pressures. Chem Eng Sci 2019;208:115149.
[50] Mienert J, Andreassen K, Posewang J, Lukas D. Changes of the hydrate stability zone of the norwegian margin from glacial to interglacial times. Acad Sci 2000;912:200–10.
[51] Mu L, Von Solms N. Hydrate thermal dissociation behavior and dissociation enthalpies in methane-carbon dioxide swapping process. J Chem Thermodynam 2018;117:33–42.
[52] Muñoz-Iglesias V, Choukroun M, Vu TH, Hodyss R, Mahjoub A, Smythe WD, Sotin C. Phase diagram of the ternary water–tetrahydrofuran–ammonia system at low temperatures. Implications for Clathrate Hydrates and Outgassing on Titan. ACS Earth Space Chem 2018;2(2):135–46.
[53] Nakagawa, R.; Hachikubo, A.; Shoji, H. Dissociation and specific heats of gas hydrate under submarine and sublacustrine environments. Proceedings of the 6th International Conference on Gas Hydrates (ICGH), Vancouver, British Columbia, Canada, July 6-10, 2008.
[54] Nasir Q, Lau KK, Lal B. Enthalpies of dissociation of pure methane and carbon dioxide gas hydrate. Int J Chem Mol Eng 2014;8:840–3.
[55] Parlouër PL, Dalmazzone C, Herzhaft B, Rousseau L, Mathonat C. Characterization of gas hydrates formation using a new high-pressure micro-DSC. J Therm Anal Calorim 2004;78:165–72.
[56] Rueff RM, Sloan ED, Yesayage VF. Heat capacity and heat of dissociation of methane hydrates. AIChE J 1988;34(9):1468–76.
[57] Sabil KM, Witkamp G-J, Peters CJ. Estimations of enthalpies of dissociation of simple and mixed carbon dioxide hydrates from phase equilibrium data. Fluid Phase Equilib 2010;290:109–14.
[58] Saw VK, Ahmad I, Mandal A, Udayabhanu G, Laik S. Methane hydrate formation and dissociation in synthetic seawater. J Nat Gas Chem 2012;21:625–32.
[59] Setzmann U, Wagner W. A new equation of state and tables of thermodynamic properties for methane covering the range from the melting line to 625 K at pressures up to 100 MPa. J Phys Chem Ref Data 1991;20:1061.
[60] Silva LPA, Dalmazzone D, Stambouli M, Lesort A, Arpentinier P, Trueba A, et al. Phase behavior of simple tetrabutylphosphine oxide (TBPO) and mixed gas (CO2, CH4 and CO2+CH4) + TBPO semiclathrate hydrates. J Chem Thermodyn 2016;102:293–302.
[61] Silva LPA, Dalmazzone D, Stambouli M, Lesort A, Arpentinier P, Trueba A, et al. Phase equilibria of semi-clathrate hydrates of tetra-n-butyl phosphonium bromide at atmospheric pressure and in presence of CH4 and CO2 + CH4. Fluid Phase Equilib 2016;413:28–35.
[62] Sloan ED, Koh C. Clathrate hydrates of natural gases. 3rd ed. Boca Raton: CRC Press; 2008.
[63] Span R, Wagner W. A new equation of state for carbon dioxide covering the fluid region from the triple-point temperature to 1100 K at pressures up to 800 MPa. J Phys Chem Ref Data 1996;25:1509.
[64] Sum AK, Burruss RC, Sloan ED. Measurement of clathrate hydrates via Raman spectroscopy. J Phys Chem B 1997;101(38):7371–7.
[65] Sun S, Hao Y, Zhao J. Analysis of gas source for the replacement of CH4 with CO2 in gas hydrate production from the perspective of dissociation enthalpy. J Chem Eng Data 2018;63:684–90.
[66] Torré, J. P.; Haillot. D.; Marlin, L.; Plantier, F.; André, R. An Innovative High Pressure Mixing Cell for Microcalorimetry: Application to Gas Hydrates. (2018) In: 16th European Conference on Mixing, 9 September 2018 – 12 September 2018 (Toulouse, France).
[67] Tsimpanogiannis IN, Michalis VK, Economou IG. Enthalpy of dissociation of methane hydrates at a wide pressure and temperature range. Fluid Phase Equil 2019;489:30–40.
[68] Udachin KA, Ratcliffe CI, Ripmeester JA. Structure, composition and thermal expansion of CO2 hydrate from single crystal x-ray diffraction measurements. J Phys Chem B 2001;105:4200–4.
[69] van der Waals JH, Platteeuw JC. Clathrate solutions. Adv Chem Phys 1959;2:1–55.
[70] Vlahakis JG, Chen H-S, Suwandi MS, Barduhn AJ. The growth rate of ice crystals: Properties of carbon dioxide hydrate, a review of properties of 51 gas hydrates, Syracuse University. Research and development report 830 prepared for US Department of Interior. 1972.
[71] Yoon J-H, Yamamoto Y, Komai T, Haneda H, Kawamura T. Rigorous approach to the prediction of the heat of dissociation of gas hydrates. Ind Eng Chem Res 2003;42:1111–4.
[72] Yu C, Fan S, Lang X, Wang Y, Li G, Wang S. Hydrogen and chemical energy storage in gas hydrate at mild conditions. Int J Hydrogen Energy 2020;45:14915–21.